Actin Polymerization and Intracellular Solvent Flow in Cell Surface Blebbing

C. Casey Cunningham

Divisions of Experimental Medicine and Hematology/Oncology, Department of Medicine, Brigham & Women's Hospital, Harvard Medical School, Boston, Massachusetts 02115

Abstract. The cortical actin gel of eukaryotic cells is postulated to control cell surface activity. One type of protrusion that may offer clues to this regulation are the spherical aneurysms of the surface membrane known as blebs. Blebs occur normally in cells during spreading and alternate with other protrusions, such as ruffles, suggesting similar protrusive machinery is involved. We recently reported that human melanoma cell lines deficient in the actin filament cross-linking protein, ABP-280, show prolonged blebbing, thus allowing close study of blebs and their dynamics. Blebs expand at different rates of volume increase that directly predict the final size achieved by each bleb. These rates decrease as the F-actin concentration of the cells increases over time after plating on a surface, but do so at lower concentrations in ABP-280 expressing cells. Fluorescently labeled actin and phalloidin injections of blebbing cells indicate that a polymerized actin structure is not present initially, but appears later and is responsible for stopping further bleb expansion. Therefore, it is postulated that blebs occur when the fluid-driven expansion of the cell membrane is sufficiently rapid to initially outpace the local rate of actin polymerization. In this model, the rate of intracellular solvent flow driving this expansion decreases as cortical gelation is achieved, whether by factors such as ABP-280, or by concentrated actin polymers alone, thereby leading to decreased size and occurrence of blebs. Since the forces driving bleb extension would always be present in a cell, this process may influence other cell protrusions as well.

EUKARYOTIC cells can extend a variety of cytoplasmic extensions from their plasma membrane surfaces that interchange or succeed one another closely. This close temporal relationship argues that, although diverse in form and size, the protrusions arise from some common etiology. Whether the different protrusions then represent different mechanisms of extension, or the same fundamental protrusive forces selectively expressed, is unknown. One protrusion in particular may be instructive. Blebs, as distinguished from the large, nonretracting blisters seen with cell injury by physical or chemical stresses (for review see 48), are spherical outpouchings of the plasma membrane that are common features at the periphery of eukaryotic cells as they spread on a substrate (3, 15, 24), or at the leading edge of moving cells (20, 30, 47). In both cases, blebs alternate with, and are ultimately replaced by, wave-like flat ruffles or small lamellopodia (6, 17, 18, 46). However, due to their spherical shape and smooth growth, blebs have long been thought to be driven by hydrodynamic forces (1, 12, 45, 46), while interpretations of what extends ruffles and lamellopodia emphasize actin polymerization (for reviews see 8, 10).

Therefore, a close study of blebs, the conditions under which they occur, and their dynamics, may provide clues to at least part of the machinery for surface extension. Such studies have been difficult to perform due to blebs' transient nature and the rapidity with which they transform into other types of protrusions (18, 46). However, we recently described three human melanoma cell lines lacking expression of an actin filament cross-linker, actin-binding protein (ABP, ABP-280) that are distinguished by markedly prolonged periods of extensive membrane blebbing in the presence of serum and physiologic temperature. This prolonged blebbing is not a feature of sublines of the ABP-280 deficient cells made to express normal ABP-280 concentrations by genetic transfection (11), arguing that changes in the cortical cytoskeleton affected by ABP-280 expression are important to blebbing. The availability of cells from lines that differ only in this regard therefore provide an ideal system to study the mechanics of blebbing and its relationship to the peripheral actin network.

This paper reports the results of such studies on membrane blebs, their characteristics, rates of expansion, and the circumstances under which they are supplanted by

Please address all correspondence to C. Casey Cunningham, Divisions of Experimental Medicine and Hematology/Oncology, Department of Medicine, Brigham & Women's Hospital, Harvard Medical School, Boston, Massachusetts 02115. Tel.: (617) 278-0321. Fax: (617) 734-2248.

© The Rockefeller University Press, 0021-9525/95/06/1589/11 $2.00

other protrusions in both the ABP-280 deficient melanoma cell lines and a variety of ABP-280 expressing cell lines. Although the duration of blebbing is markedly different among cells depending on whether they express ABP-280, the dynamics and progression of this blebbing is similar in all the types of cells studied. The findings presented here support the concept that it is the ability of a cell to efficiently form a peripheral actin gel that is a determining factor in surface protrusion, specifically postulating that blebbing occurs when the flow of intracellular solvent allowed by the cortical actin gel temporarily exceeds the ability of local actin polymerization to maintain that gel. This balance is strongly biased towards gelation, and thus decreased solvent flow, by a protein such as ABP-280, and conversely, in the ABP-280 deficient cells the flow of intracellular solvent is relatively unimpeded, resulting in more extensive blebbing. However, even in these cells, blebbing can still ameliorate over time as the fraction of polymerized actin increases to achieve a sufficiently coherent peripheral gel.

Materials and Methods

Cell Culture

All media and sera were from GIBCO-BRL (Gaithersburg, MD). The human melanoma lines M1, M2, M3, M6, A1, A2, A3, A4, and A7 were grown at 37°C and 5% CO_2 in MEM supplemented with 8% newborn calf serum and 2% FCS, as was COLO-800 (a kind gift of Dr. George Moore, Denver, CO). NIH3T3 cells (American Type Tissue Culture, Rockville, MD) were grown under the same conditions in DMEM supplemented with 10% calf serum. CHO cells were a kind gift of Dr. Robert Weiss (Brigham & Women's Hospital, Boston, MA) and were grown in DMEM with 10% calf serum.

Reagents

All reagents are from Sigma Chem. Co. (St. Louis, MO). TRITC-labeled phalloidin was diluted as a stock solution to 1 mM in DMSO and kept at −20°C. Cytochalasin D was kept as a 1-mM stock in methanol at −20°C until needed. Paraformaldehyde was prepared as a 3.7% solution in PBS (140 mM NaCl, 9 mM Na_2HPO_4, 1 mM NaH_2PO_4) and filtered before use. Ethidium bromide was prepared as a 10-mg/ml stock in water and kept sheltered from light until used.

Videomicroscopy

Cells plated on a 25-mm glass coverslip were kept at 37°C and a 5% CO_2 atmosphere on the microscope stage by means of a TC102 temperature controller and incubation chamber (Medical Systems Corp., Greenvale, NY). Differential interference contrast (DIC) and phase contrast microscopy were performed on a Zeiss Axiovert 405M inverted microscope (Carl Zeiss, Inc., Thornwood, NY) with variously a 40×, 0.9 numerical aperture (NA) Plan-neofluor, a 63×, 1.4 NA Planapochromatic, or a 100×, 1.4 NA Planapochromatic lens. For time lapse recordings, images were transmitted to a Hamamatsu C2400 video camera (Photonics Microscopy Inc., Bridgewater, NJ) and recorded on a Panasonic 6750AG video recorder (Panasonic, Secaucus, NJ). For bleb measurements a 4× collar was also placed between the microscope and camera. Recorded images from the videotape were digitized by either a QuickImage 24 frame grabber board (Mass Microsystems Inc., Sunnyvale, CA) in a Macintosh IIci computer or with the internal video acquisition capabilities of a Macintosh 840 AV computer (Apple Computer, Cupertino, CA).

Since the blebs are spherical, their volumes could then be calculated from measurements of their cross sectional area as found from a digitized bleb image with the measuring capabilities of Image 1.49 (Wayne Rasband, NIH) on a Macintosh IIci. Each measurement was repeated at least five times and the average and standard error of the mean (SEM) calculated. The accuracy of these measurements was confirmed by filming and measuring a series of latex beads of known diameter (PolySciences, Inc., Warrington, PA). If subsequent blebs arose from the initial bleb, as described in the Results section, each bleb was measured individually, even though the final structure appeared to be a single notched structure.

For determinations of the percentage of cells blebbing, a dish of cells plated for the specified time was mounted in the incubator stage and brought to 37°C. Multiple random fields were recorded until at least 100 cells had been examined in each dish and the number of cells displaying blebbing around at least 50% of the cell circumference counted. Data in the text is given as the mean number of cells blebbing ±SEM on at least 500 cells at each time point.

Microinjection

Microinjection was performed on the inverted microscope equipped with a Narishige micromanipulator and pneumatic injector (Narishige USA, Greenvale, NY). Needles were pulled on a Narishige vertical needle puller and beveled as needed on a Narishige rotating grinder. All injections were performed with the cells kept at 37°C and in a 5% CO_2 atmosphere. Injection volumes were estimated at less than 20% of total cell volume both by comparing cell images during injection and based on subsequent cell viability as previous studies suggest that cells do not survive with injection volumes greater than 15% of total cell volume (9). A series of control injections was performed with injection buffer alone in varying volumes for all experiments. TRITC-labeled phalloidin was prepared for microinjection by dilution of a 1-mM stock solution to a final concentration of 20 μM in 120 mM KCl, 10 mM Tris-Cl, pH 7.2 (injection buffer). From estimated volumes of injection, final concentration in the cell is 2–4 μM. Rhodamine-labeled actin was a generous gift of Dr. John Hartwig (Brigham & Women's Hospital) and was dialyzed at 2 mg/ml against injection buffer for 12 h, and then spun briefly at 15,000 *g* before loading for injection. Final concentration in the cell after injection was estimated at less than 5 μM.

F-Actin Determination

The average F-actin content of a population of cells was determined by two different methods. One, a modification of the method of Condeelis and Hall (7), was performed by incubating a dish of adherent cells in PHEM buffer with 0.5% Triton X-100 and 250 nM TRITC-labeled phalloidin at room temperature for 30 min. The cells were then scraped and the buffer spun at 100,000 *g* for 15 min to pellet all F-actin. After removal of the supernatant, 300 μl of methanol was added and allowed to incubate 12–48 h at −20°C. The fluorescence of each sample was then determined in a fluorimeter (Perkin-Elmer Corp., Norwalk, CT) with excitation at 540 nm and emission at 565 nm. By constructing a standard curve with readings of known amounts of TRITC-labeled phalloidin, the amount of bound F-actin could be determined per sample. Determination of the number of cells in the measured dish was found by trypsinizing a duplicate dish of cells and counting in a hematocytometer. This allowed calculation of the average F-actin content per cell.

As an alternative method, the cells were fixed, permeabilized, and stained with both TRITC-labeled phalloidin and ethidium bromide, which binds to nuclear DNA. As confirmed by staining dishes with known numbers of cells, the fluorescence intensity of ethidium remaining after washing is linearly related to cell density, if the cells are subconfluent (Fig. 1 *A*). Therefore, subconfluent 60-mm diameter plastic dishes of adherent cells were washed with PBS, then incubated with PBS with 3.7% paraformaldehyde, 0.5% Triton X-100, and 250 nM TRITC-labeled phalloidin at 37°C for 30 min. Ethidium bromide to a final concentration of 10 mM was added to the dishes and left for 5 min at room temperature. After three washings with PBS, the cells were scraped into 500 μl methanol and placed into glass cuvettes for fluorescence determination in a fluorimeter (Perkin-Elmer Corp.). The rhodamine was quantitated at an excitation at 540 nm and emission at 565 nm, while the ethidium was measured at an excitation at 525 nm and emission at 605 nm. In our hands, there is some "bleedthrough" of the ethidium fluorescence into the rhodamine wavelengths so all rhodamine measurements were corrected for this distortion. The ethidium measurements were only minimally effected by the rhodamine so no correction of these values was necessary. The average, relative F-actin content of a dish of cells could then be quantified as the ratio of the fluorescence intensities of bound TRITC-labeled phalloidin to that of bound ethidium bromide (r/e ratio).[1]

1. *Abbreviations used in this paper*: DIC, differential interference constrast; r/e ratio, ratio, ratio of rhodamine fluorescence intensity to ethidium fluorescence intensity.

To determine the extent of nonspecific binding by the TRITC portion of the labeled phalloidin in each of the above assays, the fluorescence intensity of cells from matched plates, one of which was preincubated with an excess of unlabeled phalloidin for 30 min before adding the TRITC-labeled phalloidin buffer detailed above, was compared. Less than 10% of the TRITC-labeled phalloidin remained after washing in preincubated cells.

We also employed a more direct method of comparing the F-actin content of individual cells at different stages of spreading. Trypsinized cells were plated on a scored glass coverslip mounted on the microscope stage of a Zeiss IM405 equipped for epifluorescence as above. By adding aliquots of suspended cells at various times, a population of cells on the coverslip at different stages of spreading could be viewed simultaneously. Cell count was determined by either counting a duplicate coverslip in a hematocytometer as described above, or more directly, by calculating the area viewed in one microscope field and counting the average number of cells per field for at least 20 consecutive fields. After a period of observation under phase contrast or DIC optics to determine the blebbing characteristics of each cell within the scored area, the cells were fixed and permeabilized with PBS/3.7% paraformaldehyde/0.5% Triton X-100/250 nM TRITC-labeled phalloidin. After 30 min incubation, the cells were washed with PBS and the fluorescence image of each cell at 540 nm excitation/565 nm emission recorded on videotape using a Hamamatsu C2400 camera. The gain and offset controls on the camera were kept at a constant level so that differences in fluorescence intensity could be recorded. Single frames of the videotape were digitized via the internal video frame grabber of a Macintosh 840 AV computer and processed with Image 1.49. The background pixel intensity (defined as the intensity of the field outside the cell images) was subtracted and the area and pixel intensity of each cell then measured. To demonstrate that these fluorescence intensities were linearly related to intracellular F-actin content, we constructed a standard curve of average cell fluorescence values measured in a dish of cells all of which were plated simultaneously and so were at the same stage of spreading. By beginning at initially substoichiometric, then increasing, concentrations of TRITC-labeled phalloidin added to the permeabilization buffer, the resultant increase in average fluorescence intensity could be linearly related to the amount of added TRITC-labeled phalloidin until a plateau was reached (Fig. 1 *B*). Subsequent quantitations of cell fluorescent intensities of the cells at different stages of spreading were then carried out with TRITC-labeled phalloidin concentrations above this saturating value. We again found that nonspecific binding accounted for less than 10% of the total cell fluorescence as described above.

This technique then allowed comparison of the relative F-actin contents of the cells in the scored area of the coverslip whose blebbing dynamics were known. To minimize differences in apparent actin content due to variability in this procedure, all calculated F-actin values were normalized to the average value found for at least 20 freshly plated cells, which have the least amount of F-actin, in a separate dish. This procedure was repeated with each new determination.

Results

Blebbing in ABP-280 Positive and Negative Cell Lines

Line M2 is one of three human melanoma cell lines deficient in ABP-280 protein and mRNA. A7 is a clonal subline of M2 that has restored ABP-280 expression by transfection to a level comparable to wild-type ABP-280–containing melanoma cells (11). Therefore, except for the effects of ABP-280, the cell lines are comparable in all other respects. We began by looking at differences in blebbing between these two cell lines, and most of the data will be presented as a comparison between them. However, studies were also performed in a variety of other cell lines, including the other ABP-280 deficient lines, M1 and M3, as well as other melanoma lines that express ABP-280, either natively (lines M6, M5, and COLO-800), or by transfection (lines A1, A2, and A3). In addition, some studies were repeated in blebs arising in CHO cells and NIH3T3 cells as indicated.

Occurrence of Blebbing

Cells from both M2 and A7 lines detached by either trypsinization or scraping reattach quickly within 2 h of plating on either a tissue culture–treated plastic or glass substrate. At attachment, cells from both lines are rounded in morphology and nearly 100% of cells display blebbing of the plasma membrane, dependent upon the presence of serum and physiologic (37°C) temperature (Fig. 3). As the cells begin to spread, the number displaying extensive blebbing (defined as blebbing over more than 50% of the cell circumference) decreases. However, the time required for blebbing to cease differs markedly between the two lines (Fig. 2 *A*). 4 h after plating, 43% (±7.5) of the A7 cells have stopped blebbing and have begun to display peripheral ruffles; by 8 h, less than 10% (±2) of the cells are still blebbing. In contrast, the percentage of M2 cells displaying extensive blebbing remains over 90% (±3) for over 24 h, only beginning to decrease between 36 and 48 h from plating. After 72 h, 17% (±5) of M2 cells still display extensive blebbing; however, those that have ceased blebbing become asymmetrical in shape and develop peripheral areas of relative organelle-exclusion with ruffling edges, although these ruffles are smaller than those seen in the A7 cells (Fig. 3) and, by videomicroscopy, the cells are still not motile.

F-Actin Determination

The intracellular F-actin content of the cells was quantitated at timed intervals after plating by fixation and per-

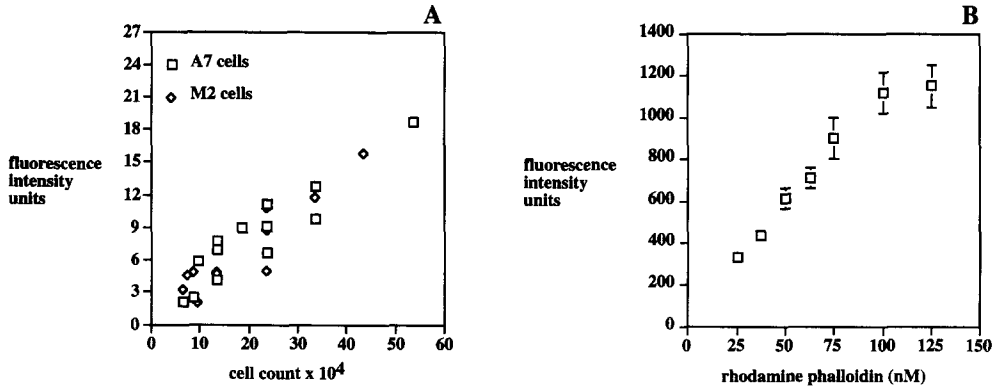

Figure 1. (*A*) The fluorescence intensity at excitation 525 nm/emission 605 nm of cells stained with 10 mM ethidium bromide is linearly related to cell number for both M2 and A7 cells. (*B*) Representative plot of the mean pixel intensity of digitized fluorescent images of permeabilized cells after incubation in increasing concentrations of rhodamine phalloidin. Bars represent standard error of the mean (SEM) of at least 25 cells digitized at each level.

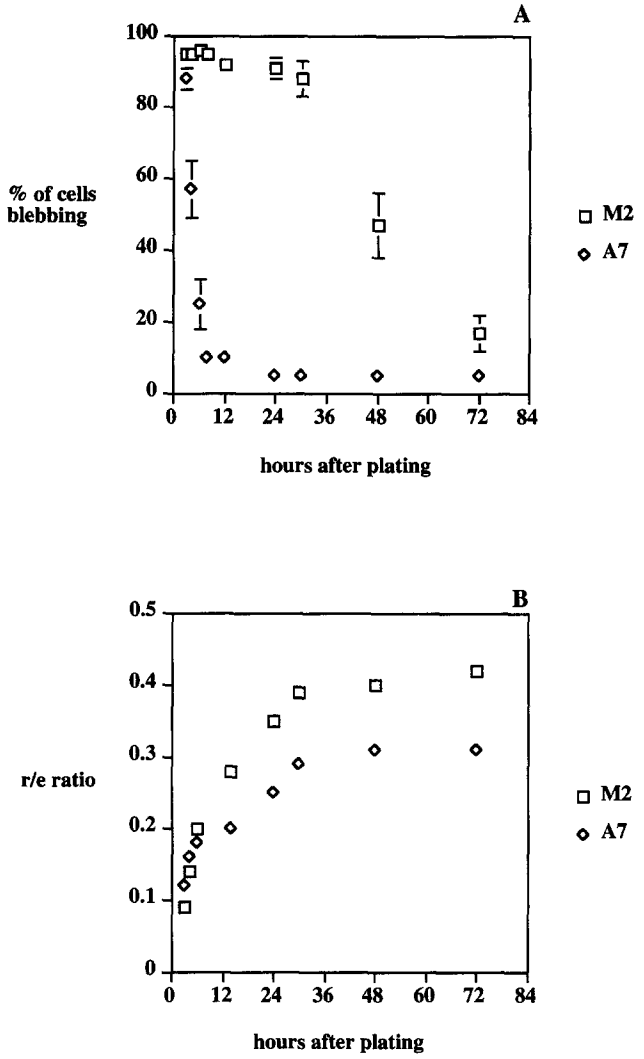

Figure 2. (*A*) Plot of the decrease in blebbing with time from plating for cells from the ABP-280 deficient line M2 and the ABP-280 expressing line A7. (*B*) Plot of average F-actin contents of M2 and A7 cells at the same times after plating as seen in *A*, expressed as ratios of fluorescence intensities of bound rhodamine phalloidin to that of bound ethidium bromide (r/e ratio).

meabilization in the presence of TRITC-labeled phalloidin, which binds F-actin stoichiometrically. The total F-actin content of a population of cells can then be determined by quantitating the fluorescence remaining in the cells after extensive washing to remove unbound phalloidin. However, since this value varies with cell density, it was corrected for differences in cell numbers at each time point by either counting the number of cells in a duplicate dish plated at the same time as the measured dish, or by incubating the cells in 10 mM ethidium bromide, which binds to nuclear DNA. As the fluorescence of the ethidium remaining after washing correlates with cell number (Fig. 1 *A*), the average F-actin content of a population of cells can be expressed as a ratio of the fluorescence intensities of bound rhodamine and ethidium, respectively (r/e ratio). Since this method is simple and reproducible, and the data consistent with that obtained by cell counting, all measurements of F-actin content are presented in this form.

At the time of attachment, cells from both lines have a similar average F-actin content (r/e ratio of 0.09–0.12) but, as they begin to spread on the substrate, this ratio increases. Quantitation of the polypeptide comigrating with purified muscle actin in Coomassie blue–stained polyacrylamide gels by quantitative densitometry indicates that the amount of total actin in the cells does not change during this period (data not shown). Total cell volume, as estimated in digitized images, also does not change over time (data not shown). Therefore, the increase in F-actin content during spreading represents a percentage change in the fraction of polymerized actin rather than an increase in total actin. The increase is particularly rapid over the first 6–12 h after attachment, but continues over the subsequent 48 h period as well. However, after the initial rapid rise in F-actin content, further increases are not as marked in cells from the A7 line, so that at each subsequent time, M2 cells have a higher r/e ratio, indicating a greater average intracellular F-actin content, than do A7 cells (Fig. 2 *B*). The "half-time" represents the time at which 50% of the cells have stopped blebbing and developed ruffling edges. Since this occurs at 3–6 h after plating for A7 cells, but not until between 30–48 h for M2 cells, the average F-actin content at this point is markedly different for the two lines (0.18 r/e for A7 vs 0.39 for M2).

These correlated processes of spreading, cessation of blebbing, development of ruffling, and increasing F-actin content can be greatly accelerated with the addition of the phorbol ester 12-O-tetradecanoyl-phorbol-13-acetate (TPA). TPA induces spreading and a rapid increase in F-actin in some cell types (34, 38, 40) and when added at 10 ng/ml to M2 cells plated 2 h previously causes an increase in their average F-actin r/e ratio from 0.10–0.41 within 30 min. Concurrent with this increase, blebbing decreases to less than 10% of cells and those cells subsequently become well spread with ruffling edges. TPA has no effect on ABP-280 mRNA or protein expression in these cells (data not shown).

Morphology and Expansion of Blebs

Although many blebs on a cell appear egg-shaped or elongated, high magnification videomicroscopy shows this shape to be the result of separate, individually spherical, membrane expansions. The development of a single bleb begins with an initial protrusion that is hemispheric in shape but rapidly becomes spherical as the height, the distance from the cell surface to the furthermost portion of the bleb wall increases (Fig. 4, *inset*). Expansion is smooth and without pause, and the base, the linear segment where the bleb joins the cell surface, usually remains constant during expansion, so that most of the bleb expansion occurs as an enlargement of the spherical shape. A bleb typically requires 4–7 s to reach full size and, after expansion ceases, a subsequent bleb often appears immediately, either from the surface of the first or at its base (Fig. 4). The expansion of the second bleb again occurs as an enlargement of a sphere from the surface of the first bleb, but the direction of bleb extension of the second bleb deviates from the axis of the first bleb (Fig. 4 *b*). A third bleb expansion at the base of the second is also possible. The result of these sequential expansions is an elongated, notched structure.

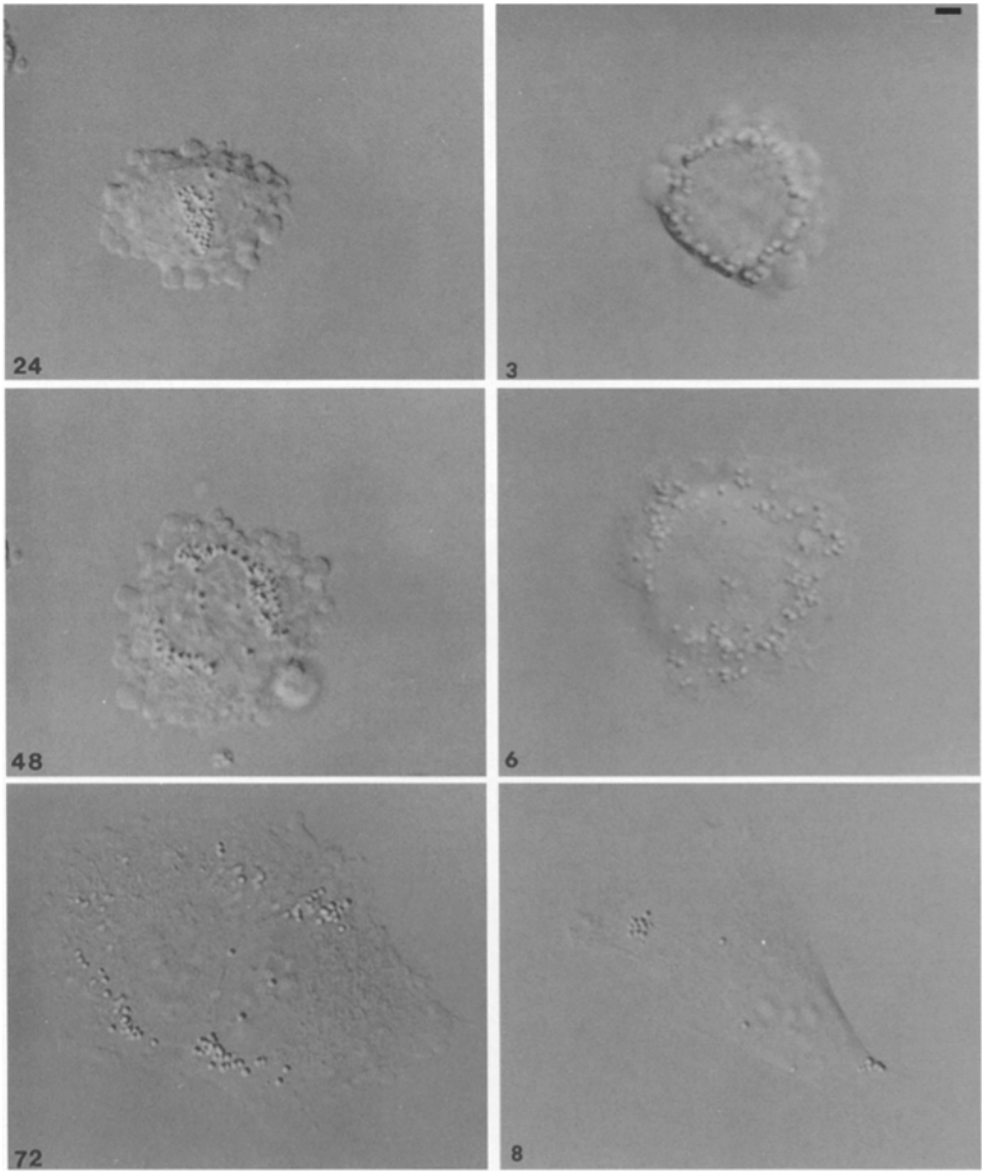

Figure 3. DIC photomicrographs of representative M2 (*left*) and A7 (*right*) cells at increasing times after plating. Numbers refer to hours after plating. Bar, 5 μm.

After reaching its full volume, each bleb remains extended for 10–20 s, then slowly retracts over 40–60 s. During retraction, the bleb surface crinkles and folds as it shrinks, in contrast to the smooth shape of expansion, and is not immediately completely resorbed into the cell surface. During retraction, some blebs, particularly those arising at the edge of spread cells, may travel centripetally on the cell surface. With the subsequent appearance of ruffles at the edge of these cells, these protrusions also move centripetally at a similar rate of speed as the previous blebs did.

Localization of G-Actin and F-Actin

Small amounts of rhodamine-labeled G-actin microinjected into blebbing M2 cells do not measurably affect the dynamics or sizes of subsequent blebs after recovery from microinjection. In the injected cells, labeled actin fluorescence appears in expanding blebs during the entire period of expansion (Fig. 5), as well as in stable and retracting blebs. In contrast, when M2 cells are microinjected with TRITC-labeled phalloidin (final concentration 2–4 μM), further extension and retraction of blebs cease quickly. In this instance, blebs extending at the time of the injection show no phalloidin staining, whereas blebs that are already fully extended at the time of injection stain brightly. The difference in labeling is particularly noticeable in instances where a second bleb is expanding from the surface of a stable bleb. Phalloidin staining appears in the stable bleb, but not in the expanding bleb (Fig. 6). There are also differences in staining in fixed, permeabilized cells, because those blebs that are expanding at the time of introduction of Triton X-100 (final concentration of 0.5%) in the fixation buffer collapse and no visible, remaining structure is seen with subsequent phalloidin staining; in contrast, stable, fully extended blebs do not collapse with permeabilization and so are consequently stained by the phalloidin.

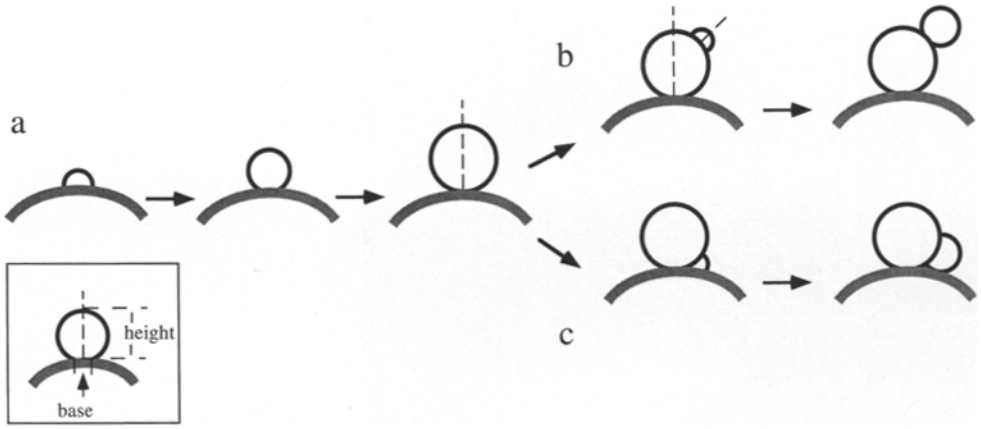

Figure 4. Cartoon illustrating the geometry of bleb expansion. A single bleb expands spherically (*a*) and then stabilizes. Frequently, a subsequent bleb appears either from the surface of the first bleb (*b*), or at its base (*c*). Dotted line is the axis perpendicular to the bleb base.

Dynamics of Bleb Expansion

Although all the bleb volumes of an individual cell remain within a twofold variation in size with each other at any one time, these volumes can vary by as much as 25-fold between different cells, or even in one cell over time. In all lines, the largest blebs are seen immediately after plating. However, after attachment to the substrate, the average volume of blebs seen in the cells begins to decrease as the cell spreads (Fig. 7). This happens after a few hours in the A7 cells, but is much more delayed in the M2 cells. Irrespective of size however, the expansion dynamics of an individual bleb remain the same. After a bleb begins, it expands at a constant rate of volume increase (Fig. 8 *A*) until stopping suddenly at the point of final volume, which can range between 5–125 cubic microns (Fig. 8 *B*). The rate at which each bleb expands shows similar variability and, as the cells spread and the average volume of their blebs becomes smaller, the rates of expansion of each of the blebs becomes smaller as well (Fig. 8 *C*). There is a striking direct proportionality between the rate of bleb expansion and the final size it attains that holds constant over the entire 25-fold range of bleb volumes seen in these two lines. Indeed, this proportionality also holds for blebs arising in all other cell lines examined, whether ABP-280 deficient (lines M1 and M3) or ABP-280 expressing, either natively (human melanoma lines M6, M5, and COLO-800), or after transfection of the cDNA for ABP-280 into the ABP-280-deficient line M2 (lines A1, A2, and A3) (Fig. 9 *A*). Further, this same relationship also describes blebs appearing in cells from other mammalian lines such as CHO and NIH3T3. In all cases, the largest blebs appear in freshly plated cells but, with spreading, blebbing not only decreases in frequency but the rates of expansion and final volumes achieved also decrease.

This linear relationship is broken, however, if actively blebbing M2 cells are treated with 0.5–1.0 micromolar cytochalasin D, which predominantly inhibits barbed end actin filament elongation. In this case, the cells continue to extend blebs for a time, but then become unable to retract

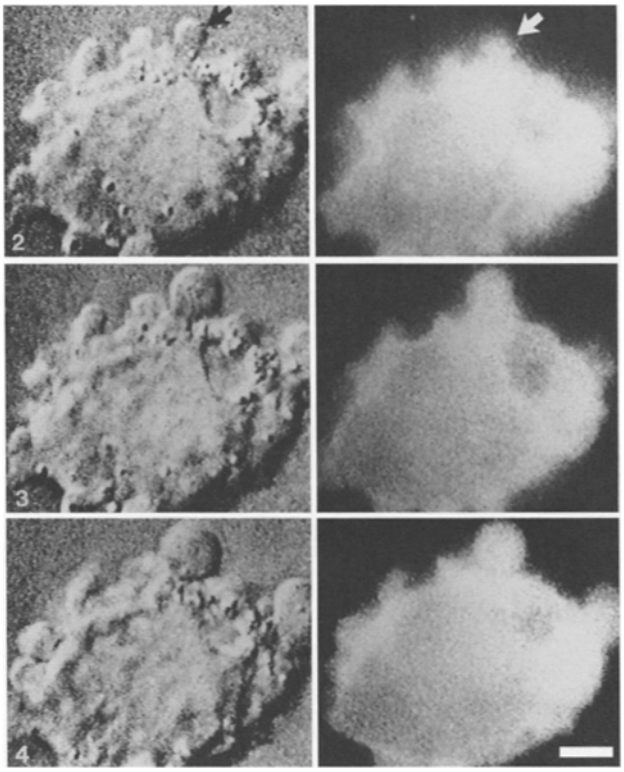

Figure 5. Sequential photomicrographs of (*left panel*) DIC and (*right panel*) fluorescence image of an M2 cell injected with rhodamine-labeled G-actin to follow actin distribution during blebbing. G-actin fluorescence is seen in a bleb (*arrow*) from the beginning of its expansion. Numbers refer to seconds after start of bleb expansion. Bar, 5 μm.

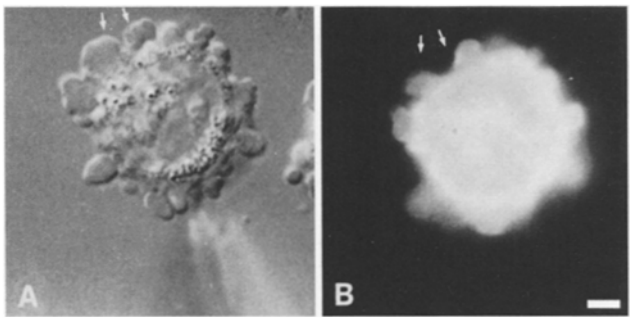

Figure 6. Photomicrographs of (*A*) DIC and (*B*) fluorescence image of an M2 cell that has just been injected with rhodamine phalloidin. Arrows mark sites where blebs were expanding just after injection. Bar, 5 μm.

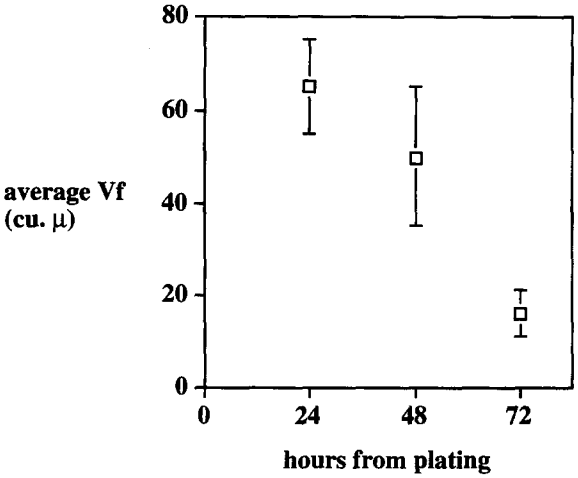

Figure 7. Plot of average bleb volume at each 24-h interval for the M2 cell pictured in Fig. 3. Bar represents the range of volumes for 15 blebs each for the 24- and 48-h time points and 8 blebs for the 72-h time.

the extended blebs, and cell surface activity ceases. Those blebs that do expand after the addition of CD grow beyond the volume predicted by their rate of expansion, i.e., these blebs no longer follow the linear correlation between rate of expansion and final volume described above (Fig. 9 *B*). The expanded blebs display a different morphology from the usual bleb, forming a translucent sphere that either detaches from the cell, or remains tethered to the surface by a slender process, and collapse with permeabilization by membrane detergents such as Triton X-100 (data not shown). Similarly, if M2 cells that are not blebbing in serum-free media are exposed to CD and then serum added after several minutes, 3–5 blebs per cell expand, but the resultant bleb volumes do not correlate with the initial rate of bleb expansion, again reaching a larger than predicted final volume.

Correlation of Individual Cell F-Actin Contents and Blebbing

Since the decrease in blebbing frequency and slower average rates of bleb expansion occurs concurrently with the increase in the average F-actin concentration as the cells spread, differences in relative F-actin content among individual M2 or A7 cells were also examined. To do this, aliquots of cells were plated at various times in one dish so that at a single time point there were populations of cells at various stages of blebbing and spreading. After recording the expansion rates and prevalence of blebs on individual cells in a marked area, the cells were then fixed and permeabilized for staining with TRITC-labeled phalloidin. Determination of individual fluorescence intensities of the fixed cells then gave a relative measure of F-actin content as described in the Materials and Methods section. There is a direct correlation between the relative intracellular F-actin concentration of a cell and the average rate of expansion, and therefore the final size, of blebs arising on that cell so that as F-actin concentration increases, the average bleb size decreases. However, this decrease occurs

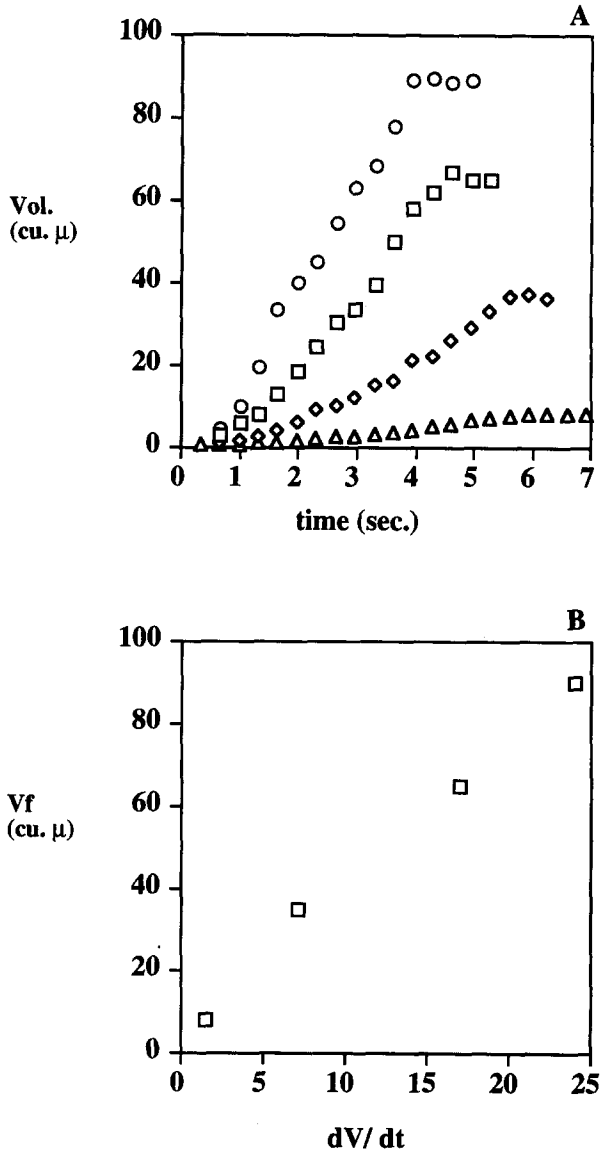

Figure 8. (*A*) Plot of volume vs time for blebs from different M2 cells showing the variability in expansion rates and final volumes achieved. Volumes in cubic microns (μ^3) are shown beginning at 0.66–1 s after the start of expansion, which is the first time point for which accurate measurements can be made. All values represent the mean of at least five measurements of the bleb and the range among the different measurements was always less than 10% of the volume. (*B*) Plot of the rate of expansion (dV/dt) vs the final volume (V_f) achieved for each of the blebs in (*A*).

much sooner, and at a lower F-actin concentration, in the ABP-280 expressing A7 cells (Fig. 10).

Discussion

Blebs were originally described in association with cell injury (for review see 48), but can also occur in noninjured cells during spreading (3, 15, 24), mitosis (4, 39), or at the leading edge of moving cells (20, 30, 47). These noninjured cell blebs are transient and frequently lead to other types of protrusions. For instance, in the deep cells of the *Fun-*

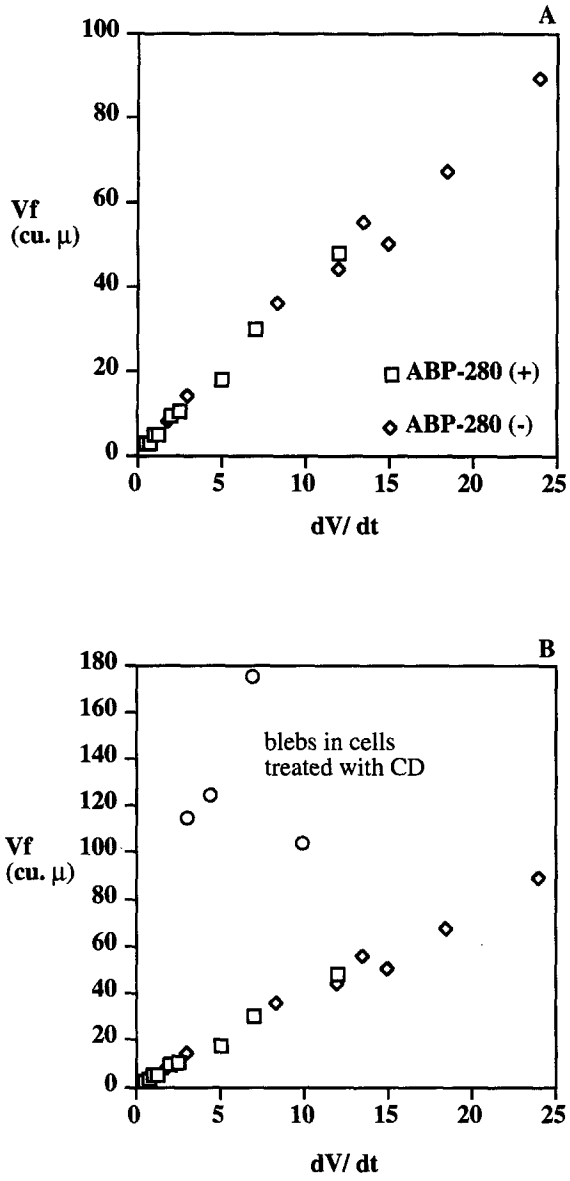

Figure 9. (*A*) Plot of dV/dt vs. V_f for blebs from both ABP-280 deficient and expressing cells showing that the correlation between the rate of expansion of a bleb and its final size holds over a wide range of expansion rates and volumes. This includes measurements of blebs in a wide array of human melanoma lines, as well as NIH3T3 and CHO cells. (*B*) Plot of dV/dt vs V_f overlaid with measurements from M2 cell blebs after incubation with cytochalasin D.

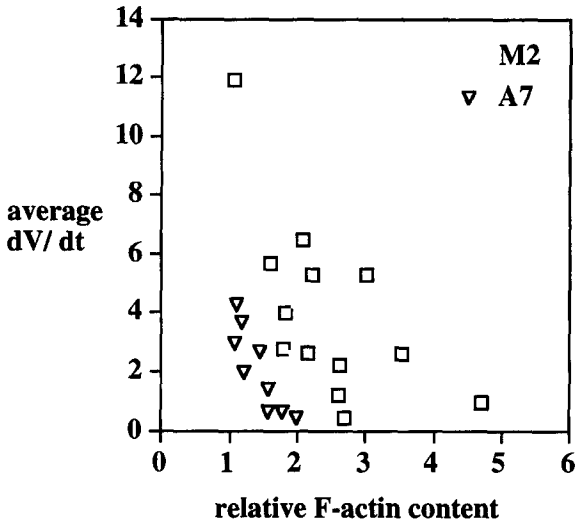

Figure 10. Plot of the relative F-actin content of individual cells vs the average rate of bleb expansions in that cell measured immediately before fixation.

dulus blastocyst elongated blebs form "lobopodia" that can alternate with, and transform into, lamellopodia (46). Ruffling replaces blebbing at the spreading cell edge (18). Such observations suggest that blebs are a constitutive feature of a certain cell state(s) (31, 42) rather than developing in response to particular signals at the cell surface (13, 19), but the precise mechanism is unclear.

One clue comes from the finding that the occurrence of blebbing during spreading is markedly prolonged in cells lacking expression of the actin gelation protein, ABP-280. This prolonged blebbing can be clearly ascribed to the effects of ABP-280 on the cell since such blebbing is diminished when ABP-280 is restored to these same cells by either transfection (lines A1, A2, A3, and A7) (11) or by microinjection (unpublished results). However, as described above, similar changes can also occur in the ABP-280 deficient cells over several days; after 2–3 d, the cells decrease or cease blebbing. This process parallels the establishment of a small cortical clear zone, a morphologic marker of peripheral network formation (33), and implies that the dynamics of blebbing are controlled by the physical state of the cortical gel.

Gels, defined as liquids immobilized by a coherent solute (2), are formed in the cell by actin polymers (32, 43). These filaments of actin can be modeled as semi-flexible rods and can reach many microns in length in vitro (29). However, in vivo, most direct measurements (22) and calculated lengths (5, 44) of actin filaments have been much shorter, less than a micron in length, although longer filaments have been measured in some cells (41). Therefore, although it is possible to achieve gel-like viscoelastic properties in the cortical cytoplasm with sufficiently concentrated long filaments from interpenetration alone (14, 27), gelation of the shorter or more dilute filaments often found in the cell requires that they be tied together by an added cross-linking molecule (16). This critical degree of impaired polymer diffusion for gelation, called the "gel point," can occur at the lowest concentrations and lengths of polymers if the linking factors that tie them together do so by orienting the actin filaments at near right angles (2, 16), as ABP-280 does (22, 23). Based on the morphological characteristics of the ABP-280 deficient cells, ABP-280 is the major actin gelation protein in these cells. However, the eventual development of manifestations of cortical gelation, i.e., peripheral organelle exclusion, in the same cells over time implies that the observed increase in intracellular concentration of F-actin is enough for gelation to finally occur due to the less efficient cross-linking provided by other filament-binding proteins that are present in

these cells (11), or from the entanglement of the concentrated filaments themselves.

How does this change in gelation affect blebbing and other protrusions? Blebs are usually posited to be fluid-based protrusions, rather than driven by the turnover of actin filaments. The findings presented above strongly support this mechanism as the driving force for bleb protrusion in that: (*1*) bleb extension is not prevented by cytochalasin D, which inhibits actin polymerization; (*2*) the bleb expansions are rapid, up to 30 μ^3/sec, so that for linear polymerization of actin in a radial progression to be responsible for extension, it requires actin assembly rates in the initial stages of bleb expansion that are much faster than have been measured in vivo (37); (*3*) injected fluorescently labeled monomeric actin is detectable at all stages of development of a bleb, while phalloidin, which binds to actin filaments, was seen only when the blebs stabilized and retracted. Although substoichiometric injections of phalloidin may be bound before reaching actin filaments distant from the site of injection (49), the fact that stable blebs which did stain were adjacent to the expanding blebs argues that the lack of staining is due to little structure in the expanding bleb. Further, actively expanding blebs collapse when permeabilized, again arguing that no significant structure exists initially.

But actin does eventually polymerize in a bleb as it matures and apparently controls bleb expansion, since inhibition of actin polymerization by cytochalasin leads to a larger bleb size. This finding then provides a model for bleb expansion which gives clues to the control exerted by the peripheral actin gel. Since each bleb expands at a constant rate of volume increase, the speed at which the bleb wall moves away from the cell surface decreases over time. Thus, if bleb expansion is stopped by polymerizing actin, originating either from the bleb wall or the cell body, finally bridging and stabilizing the spherical protrusion, then the final size of the bleb would be determined by the balance between the rate of volume expansion of an individual bleb, due to the rate of solvent flow driving that bleb's expansion, and the rate of local actin polymerization stopping expansion. As this balance shifts, blebs would expand more quickly or slowly, and achieve varying sizes, or possibly not even expand at all.

The cortical actin gel can affect this balance. Studies documenting that the total cell volume of blebbing cells or cell fragments does not increase with the expansion of a bleb (1, 15) suggest that the driving fluid flow must be from internal redistribution of solvent, rather than external uptake and, consequently, must percolate through the cortical actin network. The rate of solvent flow through the gel would then be determined by the amount of pressure, due either to gel contraction or osmotic pressure, acting against the impedance offered by the gel. Both gel contraction and osmotic pressure depend upon the state of cortical gelation; Taylor et al. provided evidence that the myosin-based contraction of an actin gel requires partial solation, as long as the gel retains sufficient network properties to permit contraction of a coherent structure (28), and similarly, the osmotic swelling pressure of a cytogel increases with partial solation of the gel (35). Of possibly more significance, however, is that Ito et al. found that the osmotically driven flow of solvent through a mixture of actin filaments slows with increasing concentrations of filaments (25) and ceases altogether at the viscometrically measured gel point (26). Thus, the establishment of a cortical actin gel could decrease the driving force for internal solvent flow, but should certainly increase the impedance offered to that flow, resulting in slower movement of fluid into a potential bleb. Any changes in the physical state of this cortical gel can then influence the rate of intracellular fluid movement, and thus the occurrence and size of the blebs extended by a cell during this time. Since there are differences in the ability of cells with and without ABP-280 to efficiently establish a cortical gel, these differences should be reflected in the occurrence and dynamics of membrane blebbing between the two types of cells. The above results support this hypothesis. There is a direct correlation between the amount of polymerized actin in the cell periphery and the occurrence and rate of expansion of membrane blebs in both ABP-280-expressing and ABP-280-deficient cells, but cessation of blebbing occurs at a much lower F-actin content when ABP-280 is present, suggesting that it is the lowered 'gel point' provided by ABP-280 that is responsible for this difference.

Interestingly, the observations above also indicate that the rate of actin polymerization should be variable among different cells, or even within the same cell at different times. There is a direct proportionality between the final bleb size and the volume expansion rate, whereas if the rate of actin polymerization was constant in cells under all conditions, the above model predicts a nonproportional relationship. Therefore, in this model, actin polymerization rates must also be affected by the structure of the peripheral actin network and change in tandem with the factors controlling the rate of bleb expansion. Although this hypothesis is speculative, if the total intracellular concentration of actin remains stable, changes in the F-actin content would reflect changes in its percentage of the total, with a corresponding inverse change in the amount of monomeric actin available for further polymerization. A cell with a decreased concentration of peripheral F-actin, and thus a decreased cortical actin gelation, would have increased local actin polymerization rates, due to an increased availability of monomer, and vice versa. These effects would be somewhat counterbalancing and could result in the observed linear relationship.

Further, in cases where polymerization reactions are impaired or completely inhibited, such as by treatment by cytochalasin D, the balance between solvent flow and polymerization rates would shift to allow a larger bleb size for that particular rate of expansion, and the rate of expansion would no longer have the same correlation with the final size of the resulting protrusion. This is again supported by the observations above. In this case, an expanding bleb would continue to grow until stopped by either diminution of the expanding force or increasing resistance to further expansion from the bleb wall and the expansion would lack any coherent internal structure. Such impairment of actin polymerization in the setting of decreased cortical gelation may then be a factor in the formation of the vesicles or blisters seen in a variety of cell injuries. These blisters would be distinguished from the dynamic blebs in both their expansion dynamics and lack of internal structure.

Finally, the machinery uncovered by this study of blebs may influence other types of cell protrusions. Cells with extensive, circumferential membrane blebbing do not extend veils or ruffles, but do so as blebbing decreases. After extension, blebs resemble protrusions such as ruffles in many respects. Retraction of the blebs is dependent upon the establishment of an actin network and is inhibited by N-ethylmaleimide (data not shown), implying that active contraction of the actin structure is involved. In spread cells, blebs can exhibit the same retrograde migration as subsequent ruffles and filopodia, again arguing that once blebs are fully formed, they are as much a part of the same cytoskeletal machinery as the other protrusions. Therefore, only the manner and form of extension is different between blebs and other protrusions and implies that signaling of the cell by chemotactic factors could lead to a variety of cell surface protrusions, depending not only upon the specific signal, but also on the state of cortical gelation of the cell at the time that signal was received. In this model, blebbing would occur in response to those signals causing partial, local solation of a portion of the cytoskeleton in the setting of overall decreased cortical gelation such that the resultant internal solvent flow rate is sufficient to outpace the local actin polymerization rate. This would occasionally occur even in cells that express ABP-280. Actin filament length directly affects the gelation of actin filaments by cross-linking proteins (21, 50), so transient changes in filament length mediated by cellular proteins that regulate actin polymerization in response to external signals could reversibly affect actin gelation in vivo, even in the presence of normal concentrations of ABP-280, and temporarily produce localized blebbing.

In cases where the flow rate of solvent is insufficient to outpace local actin polymerization, whether due to increased impedance from cortical gelation, or from an increase in the local actin polymerization rate, other forces such as osmotic gel swelling (36) might predominate, to form a lamella or other protrusion. However, even in these cases, where the flow rate of internal solvent is slowed, the hydrodynamic forces generated might still contribute to the advancement of the leading edge by forcing a rapid cycle of small extensions quickly stabilized by polymerizing actin. Thus, factors controlling both the physical characteristics of the peripheral actin network and/or the rate of actin polymerization would have effects on protrusive activity, and consequently on cell motility, by this mechanism.

I thank Drs. Thomas Stossel, Paul Janmey, Paul Dufort, Josef Käs, and George Oster for helpful discussions during this work. I also thank Ms. Elizabeth Ackerman for technical assistance.

This work was supported by grants from the National Institutes of Health CA57479, DK38452, and HL19429 (to T. P. Stossel).

Received for publication 2 February 1995 and in revised form 28 March 1995.

References

1. Albrecht-Buehler, G. 1982. Does blebbing reveal the convulsive flow of liquid and solutes through the cytoplasmic meshwork? *Cold Spring Harbor Symposia On Quantitative Biology*. 1:45–49.
2. Almdal, K., J. Dyre, S. Hvidt, and O. Kramer. 1993. Towards a phenomenological definition of the term 'Gel'. *Polymer Gels and Networks*. 1:5–17.
3. Bereiter-Hahn, J., M. Luck, T. Miebach, H. K. Stelzer, and M. Voth. 1990. Spreading of trypsinized cells: cytoskeletal dynamics and energy requirements. *J. Cell Sci.* 96:171–188.
4. Boss, J. 1955. Mitosis in cultures of newt tissues. IV. The cell surface in late anaphase and the movements of ribonucleoprotein. *Exp. Cell Res.* 8:181–197.
5. Cano, M. L., D. A. Lauffenburger, and S. H. Zigmond. 1991. Kinetic analysis of F-actin depolymerization in polymorphonuclear leukocyte lysates indicates that chemoattractant stimulation increases actin filament number without altering the filament length distribution. *J. Cell Biol.* 115: 677–687.
6. Chen, W. 1981. Surface changes during retraction-induced spreading of fibroblasts. *J. Cell Sci.* 49:1–13.
7. Condeelis, J., and A. L. Hall. 1991. Measurement of actin polymerization and cross-linking in agonist-stimulated cells. *In* Methods in Enzymology. Vol. 196. Academic Press, Inc. New York, NY. 486–496.
8. Cooper, J. A. 1991. The role of actin polymerization in cell motility. *Annu. Rev. Physiol.* 53:585–605.
9. Cooper, J. A., J. Bryan, B. d. Schwab, C. Frieden, D. J. Loftus, and E. L. Elson. 1987. Microinjection of gelsolin into living cells. *J. Cell Biol.* 104:491–501.
10. Cramer, L. P., T. J. Mitchison, and J. A. Theriot. 1994. Actin-dependent motile forces and cell motility. [Review]. *Curr. Opin. Cell Biol.* 6:82–86.
11. Cunningham, C. C., J. B. Gorlin, D. J. Kwiatkowski, J. H. Hartwig, P. J. Janmey, H. R. Byers, and T. P. Stossel. 1992. Actin-binding protein requirement for cortical stability and efficient locomotion. *Science (Wash. DC)*. 255:325–327.
12. Dipasquale, A. 1975. Locomotion of epithelial cells. Factors involved in extension of the leading edge. *Exp. Cell Res.* 95:425–439.
13. Dixon, S. J., S. Pitaru, U. Bhargava, and J. E. Aubin. 1987. Membrane blebbing is associated with Ca^{2+}-activated hyperpolarizations induced by serum and α 2-macroglobulin. *J. Cell Physiol.* 132:473–482.
14. Doi, M., and S. F. Edwards. 1986. The Theory of Polymer Dynamics. Oxford, Clarendon. 391 pp.
15. Erickson, C. A., and J. P. Trinkaus. 1976. Microvilli and blebs as sources of reserve surface membrane during cell spreading. *Exp. Cell Res.* 99:375–384.
16. Flory, P. J. 1953. Principles of Polymer Chemistry. Cornell University Press, Ithaca, New York. 672 pp.
17. Follett, E. A., and R. D. Goldman. 1970. The occurrence of microvilli during spreading and growth of BHK_{21}/C_{13} fibroblasts. *Exp. Cell Res.* 59: 124–136.
18. Forsby, N., V. P. Collins, and B. Westermark. 1985. The spreading of human normal glial and malignant glioma cells in culture. Studies on standard culture conditions. *Acta. Pathol. Microbiol. Immunol. Scand. [a].* 93: 235–249.
19. Gass, G. V., and L. V. Chernomordik. 1990. Reversible large-scale deformations in the membranes of electrically-treated cells: electroinduced bleb formation. *Biochim. Biophys. Acta.* 1023:1–11.
20. Grinnell, F. 1982. Migration of human neutrophils in hydrated collagen lattices. *J. Cell Sci.* 58:95–108.
21. Hartwig, J. H., and T. P. Stossel. 1979. Cytochalasin B and the structure of actin gels. *J. Mol. Biol.* 134:539–553.
22. Hartwig, J. H., and P. Shevlin. 1986. The architecture of actin filaments and the ultrastructural location of actin-binding protein in the periphery of lung macrophages. *J. Cell Biol.* 103:1007–1020.
23. Hartwig, J. H., and H. L. Yin. 1988. The organization and regulation of the macrophage actin skeleton. *Cell Motil. Cytoskeleton.* 10:117–125.
24. Hoglund, A. S. 1985. The arrangement of microfilaments and microtubules in the periphery of spreading fibroblasts and glial cells. *Tissue Cell.* 17: 649–666.
25. Ito, T., K. S. Zaner, and T. P. Stossel. 1987. Nonideality of volume flows and phase transitions of F-actin solutions in response to osmotic stress. *Biophys J.* 51:745–753.
26. Ito, T., A. Suzuki, and T. P. Stossel. 1992. Regulation of water flow by actin-binding protein-induced actin gelatin. *Biophys. J.* 61:1301–1305.
27. Janmey, P. A., S. Hvidt, J. Peetermans, J. Lamb, J. D. Ferry, and T. P. Stossel. 1988. Viscoelasticity of F-actin and F-actin/gelsolin complexes. *Biochemistry.* 27:8218–8227.
28. Janson, L. W., J. Kolega, and D. L. Taylor. 1991. Modulation of contraction by gelation/solation in a reconstituted motile model. *J. Cell Biol.* 114: 1005–1015.
29. Käs, J., J. Strey, and E. Sackmann. 1994. Direct imaging of reptation for semiflexible actin filaments. *Nature (Lond.).* 368:226–229.
30. Keller, H. U., A. Zimmermann, and H. Cottier. 1985. Phorbol myristate acetate (PMA) suppresses polarization and locomotion and alters F-actin content of Walker carcinosarcoma cells. *Int. J. Cancer.* 36:495–501.
31. Laskov, R., R. Baumal, and A. Polliack. 1978. Surface morphology of cultured myeloma cells: bleb formation in cell variants with defects in immunoglobulin production and secretion. *J. Reticuloendothelial Soc.* 23:361–372.
32. Luby-Phelps, K. 1994. Physical properties of cytoplasm. *Curr. Opin. Cell Biol.* 6:3–9.
33. Luby-Phelps, K., D. Lansing Taylor, and F. Lanni. 1986. Probing the structure of cytoplasm. *J. Cell Biol.* 102:2015–2022.
34. Niu, M. Y., and V. T. Nachmias. 1994. Two-step mechanism for actin poly-

merization in human erythroleukemia cells induced by phorbol ester. *Cell Motil. Cytoskeleton.* 27:327–336.
35. Oster, G. F. 1984. On the crawling of cells. *J. Embryol. Exp. Morphol.* 83: 329–364.
36. Oster, G. F., and A. S. Perelson. 1987. The physics of cell motility. *J. Cell Sci. Suppl.* 8:35–54.
37. Peskin, C. S., G. M. Odell, and G. F. Oster. 1993. Cellular motions and thermal fluctuations: the Brownian ratchet. *Biophys. J.* 65:316–324.
38. Phaire, W. L., E. Wang, and S. C. Silverstein. 1980. Phorbol myristate acetate stimulates pinocytosis and membrane spreading in mouse peritoneal macrophages. *J. Cell Biol.* 86:634–640.
39. Porter, K. R., D. Prescott, and J. Frye. 1973. Changes in the surface morphology of Chinese hamster ovary cells during the cell cycle. *J. Cell Biol.* 57:815–836.
40. Sheterline, P., J. E. Rickard, B. Boothroyd, and R. C. Richards. 1986. Phorbol ester induces rapid actin assembly in neutrophil leucocytes independently of changes in [Ca^{2+}] and pH. *J. Muscle Res. Cell Motil.* 7:405–412.
41. Small, J. V. 1995. Getting the actin filaments straight: nucleation-release or treadmilling? *Trends Cell Biol.* 5:52–55.
42. Sugrue, S. P., and E. D. Hay. 1981. Response of basal epithelial cell surface and cytoskeleton to solubilized extracellular matrix molecules. *J. Cell Biol.* 91:45–54.
43. Taylor, D. L., P. L. Moore, J. S. Condeelis, and R. D. Allen. 1976. The mechanochemical basis of amoeboid movement. I. Ionic requirements for maintaining viscoelasticity and contractility of Amoeba cytoplasm. *Exp. Cell Res.* 101:127–133.
44. Theriot, J. A., and T. J. Mitchison. 1991. Actin microfilament dynamics in locomoting cells [see comments]. *Nature (Lond.).* 352:126–131.
45. Tickle, C., and J. P. Trinkaus. 1977. Some clues as to the formation of protrusions by Fundulus deep cells. *J. Cell Sci.* 26:139–150.
46. Trinkaus, J. P. 1973. Surface activity and locomotion of *Fundulus* deep cells during blastula and gastrula stages. *Dev. Biol.* 30:69–103.
47. Trinkaus, J. P. 1980. Formation of protrusions of the cell surface during tissue cell movement. *Prog. Clin. Biol. Res.* 41:887–906.
48. Trump, B. F., B. P. Croslev, and W. J. Mergner. 1971. *In* Cell Membranes: Biological and Pathological Aspects. G. W. Richter and D. G. Scarpelli, editors. Williams and Wilkins, Baltimore. 84–126.
49. Wang, Y. L. 1987. Mobility of filamentous actin in living cytoplasm. *J. Cell Biol.* 105:2811–2816.
50. Yin, H. L., K. S. Zaner, and T. P. Stossel. 1980. Ca^{2+} control of actin gelation. Interaction of gelsolin with actin filaments and regulation of actin gelation. *J. Biol. Chem.* 255:9494–9500.